Emergence of collective motion in a model of interacting Brownian particles

Victor Dossetti[1, 2, *] and Francisco J. Sevilla[3, †]

[1] *Instituto de Física, Benemérita Universidad Autónoma de Puebla, Apdo. Postal J-48, Puebla 72570, Mexico*
[2] *Consortium of the Americas for Interdisciplinary Science, University of New Mexico, Albuquerque, NM 87131, USA*
[3] *Instituto de Física, Universidad Nacional Autónoma de México, Apdo. Postal 20-364, 01000, México D.F., Mexico*

(ΩDated: July 1, 2015)

By studying a system of Brownian particles, that interact among themselves only through a local velocity-alignment force that does not affect their speed, we show that self-propulsion is not a necessary feature for the flocking transition to take place as long as underdamped particle dynamics can be guaranteed. Moreover, the system transits from stationary phases close to thermal equilibrium, with no net flux of particles, to far-from-equilibrium ones exhibiting collective motion, phase coexistence, long-range order and giant number fluctuations, features typically associated to ordered phases of models where self-propelled particles with overdamped dynamics are considered.

PACS numbers: 87.10.-e, 05.70.Fh, 05.40.-a, 05.70.Ln

Collective motion is an ubiquitous phenomenon in biological groups such as flocks of birds, schools of fishes, swarms of insects, etc. The study of these far-from-equilibrium systems has attracted great interest over the last few decades, as the spontaneous emergence of such ordered phases and coordinated behavior, arising from local interactions, cannot be accounted for by the standard theorems of equilibrium statistical mechanics [1].

Introduced twenty years ago, the seminal model by Vicsek *et al.* (VM) [2] provided a simple approach to study the transition to collective motion, in a non-equilibrium situation, considering two basic ingredients: *self-propelled* particles (SPP) and a local velocity-*alignment* interaction among them. Discrete in nature, particles instantaneously orient their motion along the average direction of motion of their neighbors within a radius R, while stochastic perturbations are considered by adding a random angle (*"noise"*) to this direction. In two dimensions, a complete phase diagram for the VM has recently been presented and explained in terms of a liquid-gas transition [3], ultimately proving the discontinuous character of the transition to collective motion in this model [4]. In [3], three distinct phases have been identified: a disordered gas at high noise and low density, an intermediate (coexistence) region where a smectic arrangement of ordered bands travel in a disordered background, and a homogeneous polar liquid at low noise and high density (also known as the "Toner-Tu" phase) [5]. The latter is characterized by collective motion with *long-range order* and *giant number fluctuations* [3, 4], the hallmark of a non-equilibrium dynamics. This is the reason why the VM can be considered as a paradigm of non-equilibrium phase transitions, as such ordered phases are forbidden in equilibrium (for Heisenberg-like models) by the Mermin-Wagner-Hohenberg theorem (MWHT) [6].

The VM has inspired many different models over the years [7–9], where self-propulsion has been kept as an essential ingredient for the transition to collective motion to take place, in combination with interactions of the "social" type among the particles such as velocity-alignment. This has led to the development of sophisticated nonlinear friction terms [10, 11], a bias that may be justified by arguing that the concept of self-propelled (or *active* Brownian) particles captures the natural ability (seen in biological and in man-made systems) for the agents to develop motion by themselves [12, 13] and, additionally, that it is an important ingredient for pattern formation in models of collective motion [14].

In this Letter, we study the emergence of collective motion in a two-dimensional system of N *passive* Brownian particles that interact among themselves only through a local velocity-aligning force, that affects only the particles' direction of motion, avoiding any propelling effect from it. We show that the symmetry breaking of the disordered phase corresponds to the breakdown of a close-to-equilibrium state for a particular value of the ratio between two characteristic time-scales in the system: one related to the mean collision time of Brownian particles immersed in a thermal bath, and the other to the rate of alignment among particles. Our results show that self-propulsion is not a necessary feature for the development of collective motion with true long-range order, whenever underdamped particles, for which inertial motion cannot be neglected, are considered. Through a standard numerical analysis, the far-from-equilibrium nature of these states is established, as they exhibit the typical features associated with this kind of phases.

Our model is described in terms of generic stochastic differential equations for Brownian particles restricted to move within a box of linear size $\mathcal{L}$ with periodic boundary conditions, *i.e.*,

$$m\frac{d\boldsymbol{v}_i}{dt} = \boldsymbol{\mathcal{F}}_i - \gamma\boldsymbol{v}_i + \boldsymbol{\xi}_i, \tag{1}$$

where $\boldsymbol{v}_i = d\boldsymbol{x}_i/dt$ and m is the mass of the particles.

The last two terms on the right hand side correspond to the linear-dissipative and fluctuating forces that appear in the Langevin description of Brownian motion, respectively. The components of the vector $\boldsymbol{\xi}_i$ are uncorrelated Gaussian white noises with zero mean and, assuming the fluctuation-dissipation relation (FDR) to be valid, with autocorrelation function $\langle \xi_{i,\mu}(t)\xi_{j,\nu}(t')\rangle = 2\gamma k_B T \delta_{i,j}\delta_{\mu,\nu}\delta(t-t')$, where $\xi_{i,\eta}$ is the η-th Cartesian component of $\boldsymbol{\xi}_i$, k_B is the Boltzmann constant, T the temperature of the bath, whereas $\delta_{u,w}$ and $\delta(\tau)$ are the Kronecker's and Dirac's delta functions, respectively.

The alignment action is implemented through the force $\boldsymbol{\mathcal{F}}_i = \Gamma\left[\boldsymbol{f}_i - \hat{\boldsymbol{v}}_i\left(\boldsymbol{f}_i\cdot\hat{\boldsymbol{v}}_i\right)\right]$, that corresponds to the two-dimensional form of $\Gamma\left[\hat{\boldsymbol{v}}_i\times\left(\boldsymbol{f}_i\times\hat{\boldsymbol{v}}_i\right)\right]$, with $\hat{\boldsymbol{v}}_i$ being the unitary vector in the direction of $\boldsymbol{v}_i$ and $v_i = |\boldsymbol{v}_i|$, while $\boldsymbol{f}_i = \left[N_R(i)\right]^{-1}\sum_{j|\boldsymbol{x}_j\in\Omega_R(\boldsymbol{x}_i)}\hat{\boldsymbol{v}}_j$ corresponds to the arithmetic average of the direction of motion of the $N_R(i)$ particles that surround the i-th particle within a neighborhood $\Omega_R(\boldsymbol{x}_i)$ of radius R. The coupling factor Γ is a measure of how fast the velocity vector of a single particle aligns along the direction of $\boldsymbol{f}_i$. It is easy to check its non-propelling character since $\boldsymbol{\mathcal{F}}_i\cdot\hat{\boldsymbol{v}}_i = 0$. This alignment interaction corresponds to a simple finite-rate generalization of the one introduced in [2], although finite-rate alignment interactions have been considered before in some other forms [11, 13, 15].

It is instructive to rewrite (1) in polar coordinates, *i.e.*,

$$m\frac{dv_i}{dt} = -\gamma v_i + \frac{k_B T\gamma}{m}\frac{1}{v_i} + \xi_{v_i}, \tag{2a}$$

$$mv_i\frac{d\varphi_i}{dt} = \frac{\Gamma}{N_R(i)}\sum_{j|\boldsymbol{x}_j\in\Omega_R(\boldsymbol{x}_i)}\sin[\varphi_j-\varphi_i] + \xi_{\varphi_i}, \tag{2b}$$

where $d\boldsymbol{x}_i/dt = v_i\hat{\boldsymbol{v}}_i$, $\boldsymbol{v}_i = v_i e^{i\varphi_i}$, and ξ_{v_i} and ξ_{θ_i} are independent Gaussian white noises, both with autocorrelation function $2k_BT\gamma\delta(t-s)$ and computed from $\boldsymbol{\xi}_i$ through the transformation $\xi_{v_i} = \xi_{i,x}\cos\varphi_i + \xi_{i,y}\sin\varphi_i$ and $\xi_{\varphi_i} = \xi_{i,x}\sin\varphi_i + \xi_{i,y}\cos\varphi_i$ [16]. The second term in (2a) proportional to k_BT, that comes from the Ito's calculus when switching to polar coordinates [16], makes explicit that it is a *"thermal propulsion"* and not self-propulsion that is acted upon the particle speed.

In its polar form (2), our model is suitable to be generalized, as self-propulsion terms and active fluctuations [17] can easily be considered. Moreover, in the overdamped-*alignment* limit, *i.e.*, when $\Gamma\to\infty$, (2b) turns into the instantaneous alignment rule of the VM and a perfectly ordered phase is expected as it occurs in that model in the absence of the *non-thermal* angular noise. Also, self-propulsion can be incorporated into (2a) by replacing the constant friction coefficient γ with a nonlinear speed-dependent $\gamma(v_i)$, so that the new term $-\gamma(v_i)v_i$ would be able to keep particle speeds around a fixed value $v_{\rm sp}$ [13, 18]. In the overdamped-*speed* limit, *i.e.*, when the latter is characterized by dynamics faster than others in the system, the speed of the particles can directly be set to a constant $v_{\rm sp}$ and (2a) disregarded.

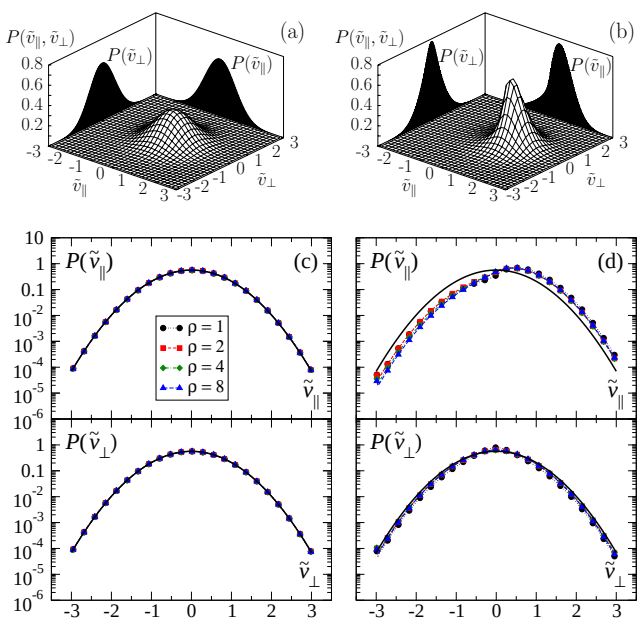

FIG. 1: (Color online) Stationary probability distribution $P(\tilde{v}_\parallel,\tilde{v}_\perp)$ of the individual velocity of the particles, $\tilde{\boldsymbol{v}}_i(=\boldsymbol{v}_i/v_0)$, projected along the direction of the mean velocity of the group, $\tilde{v}_\parallel$, and in the transversal one, $\tilde{v}_\perp$, for a subcritical $\tilde{\Gamma}=1$ in (a) and a supercritical $\tilde{\Gamma}=8$ in (b) for systems with $\rho=1$ and $L=96$. The distributions in the vertical planes correspond to the integral of $P(\tilde{v}_\parallel,\tilde{v}_\perp)$ over $\tilde{v}_\parallel$ and $\tilde{v}_\perp$, yielding $P(\tilde{v}_\perp)$ and $P(\tilde{v}_\parallel)$, respectively. In (c) and (d), log-lin plots of $P(\tilde{v}_\parallel)$ and $P(\tilde{v}_\perp)$ for systems with $L=272$ and $\rho=1,2,4,8$: in (c) for subcritical disordered states with $\tilde{\Gamma}=3, 2.9, 2.5, 2.28$, respectively, and in (d) for ordered states with $\langle\Lambda\rangle\approx 0.46$. The solid black curves correspond to the equilibrium Maxwell-Boltzmann distribution.

We choose as time, speed and length scales the quantities: $\tau_0 = m/\gamma$, $v_0 = \sqrt{2k_BT/m}$ and $r_0 = v_0\tau_0$, respectively. In this way, the number of independent parameters in our model is reduced to three: the dimensionless alignment-coupling constant $\tilde{\Gamma} = v_0^{-1}\gamma^{-1}\Gamma$, the dimensionless interaction range R/r_0, and the dimensionless particle density $\rho = N/L^2$ with $L = \mathcal{L}(R/r_0)$. Without loss of generality, we fix $R/r_0 = 1$ further on. As well, our numerical results were obtained by integrating equations (1) using a modified velocity-Verlet algorithm [19] with an integration time-step $\Delta t = 0.01$. Uniform random initial conditions where taken for the particle positions, while initial velocities where drawn from the equilibrium Maxwell-Boltzmann velocity distribution.

In the absence of interactions ($\tilde{\Gamma}=0$), the particle dynamics is constrained by the FDR as in the standard description of Brownian motion, therefore, the stationary-state distribution of the single-particle velocities corresponds to that of equilibrium with the high-

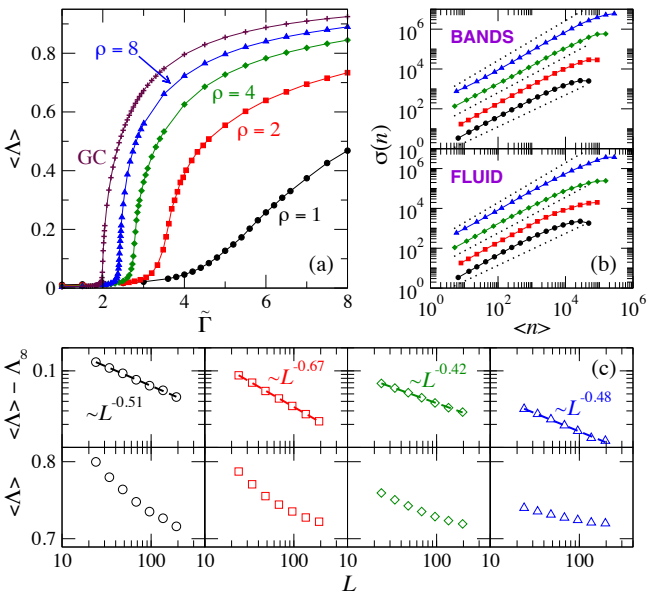

FIG. 2: (Color online) (a) Stationary order parameter $\langle\Lambda\rangle$ vs $\tilde{\Gamma}$ for systems with $L = 96$ and different density values. The curve with plus symbols corresponds to the globally-coupled (GC) case for a system with $\rho = 1$ and $L = 320$. (b) Giant density fluctuations, $\sigma(n)$ vs $\langle n\rangle$, for ordered phases with *bands* (top: $0.2 < \langle\Lambda\rangle < 0.5$) and in the *fluid* phase (bottom: $\langle\Lambda\rangle \approx 0.8$) of systems with $L = 272$. The dotted lines have slopes 0.8, 0.9 and 1 from bottom to top. (c) In the bottom row, log-log plots of $\langle\Lambda\rangle$ vs L for systems with $\rho = 1, 2, 4, 8$ and $\tilde{\Gamma} = 18, 8, 5, 4$ from left to right. The log-log plots of the top row show the same data from which $\Lambda_\infty = 0.669538, 0.698997, 0.689226, 0.706573$ has been respectively subtracted. The dashed lines correspond to power-law-decay fits, with fitting error smaller than 2%.

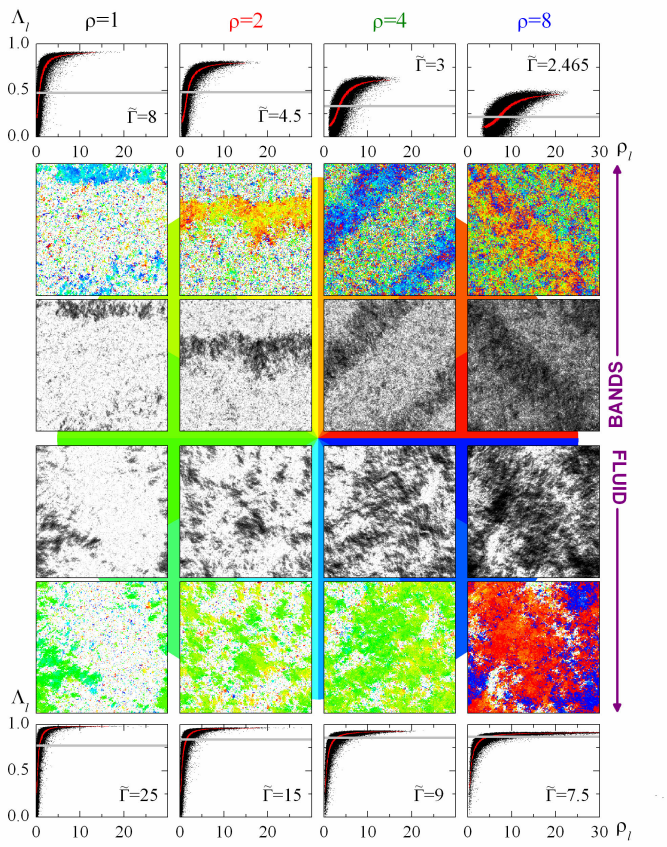

FIG. 3: In the first and last rows, scatter plots of the local oder parameter Λ_l versus the local density ρ_l computed in boxes of size $l = 14$ for the systems of figure 1(b). The red lines passing through the middle of the scattered black dots are running averages in a local window in ρ_l. The horizontal grey line corresponds to the stationary order parameter $\langle\Lambda\rangle$. The third and fourth rows show snapshots of corresponding density fields (the darker gray level represents higher particle density), while their direction fields are shown in the second and fifth rows, respectively. The underlying circular color key shows the local direction of motion.

est rotational symmetry. Interestingly, for smaller values than that of a threshold, $\tilde{\Gamma}_c$, when the alignment time-scale is larger than that related to the FDR, the system remains in a close-to-equilibrium phase still characterized by properties of *thermal equilibrium* with no net transport, normal diffusion of individual particles and Maxwellian probability densities of single-particle velocities [Figs. 1(a) and 1(c)]. In particular, notice that the stationary probability distributions $P(\tilde{v}_\parallel)$ and $P(\tilde{v}_\perp)$ (broken curves with symbols) in Fig. 1(c), are indistinguishable form the equilibrium Maxwell-Boltzmann distribution for interactionless particles with a nominal temperature T (solid black curves). In this case, thermal fluctuations preclude the development of any correlations among the particles' velocities. Indeed, orientation correlations that may emerge within the time between two successive collisions, due to the alignment interaction, are randomized by noise, thus preventing the spontaneous breaking of a continuous symmetry as established by the MWHT for equilibrium [20].

As $\tilde{\Gamma}$ increases above $\tilde{\Gamma}_c$, alignment dynamics become faster than those associated with the FDR, *rectifying* the thermal fluctuations into collectively directed motion, even though no self-propulsion is individually exerted on the particles. This mechanism has no analogue in models studied by equilibrium statistical mechanics, thus, it can be considered as the essential ingredient that escapes from the scope of the MWHT. Consequently, the system develops complex, self-induced, far-from-equilibrium phases that exhibit net flux of particles and non-Maxwellian probability densities of single-particle velocities [Fig. 1(b) and 1(d)].

We monitor the transition from the disordered gas phase to out-of-equilibrium states through the accumulated order parameter $\langle\Lambda\rangle = \lim_{\mathcal{T}\to\infty} \mathcal{T}^{-1} \int_0^{\mathcal{T}} \Lambda(t)\, dt$, that is calculated from the instantaneous $\Lambda(t) = |N^{-1} \sum_{i=1}^{N} e^{i\varphi_i(t)}|$ with $\varphi_i(t)$ defined as before. The critical point $\tilde{\Gamma}_c$ that separates the disordered and ordered

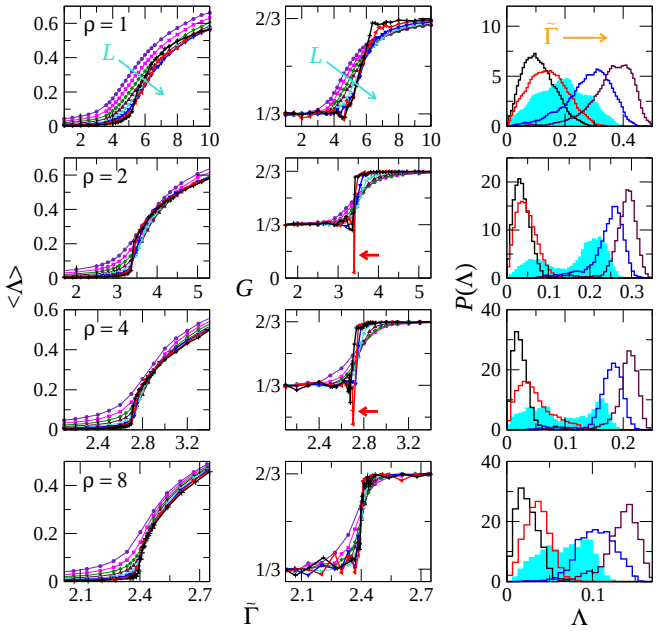

FIG. 4: (Color online) Left column, stationary order parameter $\langle\Lambda\rangle$ vs $\tilde{\Gamma}$ for systems with increasing L (L = 24, 34, 48, 68, 96, 136, 192, 272). Middle column, plots of the Binder cumulant G vs $\tilde{\Gamma}$ for the same systems on the left. As can be appreciated, the curves $\langle\Lambda\rangle$ vs $\tilde{\Gamma}$ with largest L (red and black curves) start to overlap the rest, while G starts to show a singularity around the critical point for some of the systems, marked with short horizontal arrows. For these cases, the stationary $P(\Lambda)$ vs Λ, shown on the right column for systems with $L = 192$ and for different values of $\tilde{\Gamma}$, shows a clear bimodal shape (filled curves) around the critical point. All of these facts evidence a discontinuous phase transition.

phases decreases with ρ, reaching the limit value $\tilde{\Gamma}_c \approx 2$ when $\rho \to \infty$ and/or $R \to \mathcal{L}$, the latter corresponding to the globally-coupled (GC) regime [Fig. 2(a)]. Surprisingly, even though we only consider "thermal-propulsion" and velocity alignment, without self-propulsion as explained before, our model exhibits true *long-range order* as shown in Fig. 2(c), where the order parameter $\langle\Lambda\rangle$ slowly decays (algebraically) with L to a constant value $\Lambda_\infty > 0$ for all of the values of ρ considered.

Regarding the ordered phases of our model, we have been able to identify at least two [Fig. 3] in analogy with [3]: a coexistence region just above $\tilde{\Gamma}_c$, where ordered bands travel in a disordered background, and a homogeneous polar liquid at higher $\tilde{\Gamma}$ values, similar to the "Toner-Tu" phase [5]. These ordered phases exhibit the typical features of far-from-equilibrium ordered phases present in models that consider SPP. To say, our model shows *giant number fluctuations*, that is a signature of fluctuating ordered active phases, characterized by $\sigma(n)$, corresponding to the square root of the variance of the particles contained in square boxes of linear size l with respect to the average value $n = \rho l^2$. For our model, even though $\sigma(n)$ scales like n^α with $\alpha > \frac{1}{2}$ for both of these phases, as illustrated in Fig. 2(b), they do not seem to present the scaling exponents known by their counterparts in SPP models. For instance, in the coexistence region, where traveling ordered *bands* are observed, an exponent $\alpha = 1$ is expected for clustered phases up to $l < L$ [21], while we record an exponent $\alpha \approx 0.9$ [top panel of Fig. 2(b)]. This behavior may be attributed to finite-size-effects [22], as it is up to $L \approx 200$ that we start to clearly observe these structures. Less trivial is the case for our homogeneous *fluid* phase, where an exponent $\alpha = \frac{4}{5}$ is expected for models that consider SPP [9]. In our case, the scaling observed is clearly larger than that, up to a threshold, beyond which density-fluctuations start to scale with a slope below that value [bottom panel of Fig. 2(b)]. This threshold moves to higher values in $\langle n\rangle$ as ρ increases. Therefore, our results may also hint that density fluctuations coming from an *underdamped dynamics* (as the one considered here) are qualitatively different from those found in SSP models with an *overdamped dynamics*. In fact, the ordered bands in the coexistence phase of our model seem less sharp and dense than those displayed, for instance, by the VM [3, 4]. Clearly, further studies are required to elucidate this discrepancy.

Additionally, whenever interactions depend on the distance, far-from-equilibrium ordered phases exhibit a strong coupling between *local density and local order* [4, 9]. This is illustrated in the top and bottom rows of Fig. 3, for the coexistence and homogeneous phases of our model, respectively, being more evident for dilute more-segregated systems. For these, particles tend to concentrate in a few structures. This behavior decreases with ρ as the system becomes more homogeneous in both phases. See, for example, that the snapshots for the direction field (second and fifth rows) show less white spots as ρ increases, meaning that, wherever there is color, there are at least a few particles. In fact, as $\rho \to \infty$ or in the GC regime, this feature allows for the analytical treatment of the model where the instability of the disordered close-to-equilibrium state can be demonstrated, and the relation of our model to the Kuramoto model of synchronization is revealed [23].

Lastly, Fig. 4 shows results regarding the transition to collective motion for our model. On the left column, $\langle\Lambda\rangle$ is plotted vs $\tilde{\Gamma}$ for systems with increasing size. Notice how the curves with largest L start to overlap the rest. For $\rho = 2, 4$, their corresponding Binder cumulant $G = 1 - \langle\Lambda^4\rangle/(3\langle\Lambda^2\rangle^2)$, in the middle column, starts to show clear signs of discontinuity around the critical point, while their stationary $P(\Lambda)$ on the right becomes bimodal through the transition point, confirming the phase segregation. These facts evidence a discontinuous phase transition (see [3] and references therein). We must mention that dilute systems show stronger fluctuations in $\Lambda(t)$, requiring longer integration times than systems with a larger ρ (our runs for the largest dilute systems consid-

ered about 10^8 integration steps).

In summary, our results show that local non-Hamiltonian interactions that do not preserve momentum (such as the alignment interaction typically used to model flocking behavior), in combination with an underdamped particle dynamics, are the only key ingredients for the Vicsek transition to take place. Thus, self-propulsion is an unnecessary feature for systems to develop long-range order, out of local interactions, as is typically assumed for active systems. Moreover, our model shows all of the phenomenology of the VM class, in addition to the close-to-equilibrium character of the disordered gas phase and the anomalous scaling of the density fluctuations in the ordered ones. These features make our model suitable for studying the passage from states where entropy is maximized to stationary phases where entropy is produced (this has already been done in the GC regime of our model [24]). Finally, our model may provide yet another tool, due to its lack of self-propulsion, for the study of the development, stability and interaction of the traveling ordered bands observed in the coexistence phase, as well as for the study of giant density fluctuations. We believe that all of these aspects might be of interest beyond the field of active matter.

The authors gratefully acknowledge the computing time granted on the supercomputers MIZTLI (DGTIC-UNAM), THUBAT-KAAL (CNS-IPICyT) and, through the project "Cosmología y astrofísica relativista: objetos compactos y materia obscura", on XIUHCOATL (CINVESTAV). V.D. acknowledges support from the grant PROMEP/103.5/10/7296 and from CONACyT. F.J.S. acknowledges support from the grant PAPIIT-IN113114.

* Electronic address: dossetti@ifuap.buap.mx; author to whom correspondence should be addressed.
† Electronic address: fjsevilla@fisica.unam.mx

[1] T. Vicsek and A. Zafeiris, Phys. Rep. **517**, 71 (2012).
[2] T. Vicsek, A. Czirók, E. Ben-Jacob, I. Cohen, and O. Shochet, Phys. Rev. Lett. **75**, 1226 (1995).
[3] A. P. Solon, H. Chaté, and J. Tailleur, Phys. Rev. Lett. **114**, 068101 (2015).
[4] G. Grégoire and H. Chaté, Phys. Rev. Lett. **92**, 025702 (2004); H. Chaté, F. Ginelli, G. Grégoire, and F. Raynaud, Phys. Rev. E **77**, 046113 (2008).
[5] J. Toner and Y. Tu, Phys. Rev. Lett. **75**, 4326 (1995); J. Toner and Y. Tu, Phys. Rev. E **58**, 4828 (1998); J. Toner, Y. Tu, and S. Ramaswamy, Ann. Phys. (N.Y.) **318**, 170 (2005); J. Toner, Phys. Rev. E **86**, 031918 (2012).
[6] N. D. Mermin and H. Wagner, Phys. Rev. Lett. **17**, 1133 (1966); P. C. Hohenberg, Phys. Rev. **158**, 383 (1967); N. D. Mermin, J. Math. Phys. **8**, 1061 (1967).
[7] D. S. Calovi, U. Lopez, S. Ngo, C. Sire, H. Chaté, and G. Theraulaz, New J. Phys. **16**, 015026 (2014).
[8] T. Ohta and S. Yamanaka, Eur. Phys. J. Special Topics **223**, 1279 (2014).
[9] F. Ginelli and H. Chaté, Phys. Rev. Lett. **105**, 168103 (2010).
[10] U. Erdmann, W. Ebeling and V. S. Anishchenko, Phys. Rev. E **65**, 061106 (2002); U. Erdmann, W. Ebeling and A. S. Mikhailov, Phys. Rev. E **71**, 051904 (2005).
[11] V. Dossetti, F. J. Sevilla and V. M. Kenkre, Phys. Rev. E **79**, 051115 (2009).
[12] F. Schweitzer, *Brownian Agents and Active Particles: Collective Dynamics in the Natural and Social Sciences* (Springer-Verlag, Berlin, 2007).
[13] R. Grossmann, L. Schimansky-Geier and P. Romanczuk, New J. Phys. **14**, 073033 (2012).
[14] N. Shimoyama, K. Sugawara, T. Mizuguchi, Y. Hayakawa, and M. Sano, Phys. Rev. Lett. **76**, 3870 (1996); W. Ebeling and U. Erdmann, Complexity **8** (4), 23-30 (2003); J.R. Touma, A. Shreim, and L.I. Klushin, Phys. Rev. E **81**, 066106 (2010).
[15] A. Mogilner and L. Edelstein-Keshet, Physica D **89** 346 (1996); C. R. McInnes, Phys. Rev. E **75**, 032904 (2007); F. D. C. Farrell, M. C. Marchetti, D. Marenduzzo, and J. Tailleur, Phys. Rev. Lett. **108** 248101 (2012).
[16] C. W. Gardiner, *Handbook of Stochastic Methods for Physics, Chemistry and the Natural Sciences* (Springer, Berlin, 1997).
[17] P. Romanczuk and L. Schimansky-Geier, Phys. Rev. Lett. **106**, 230601 (2011).
[18] P. Romanczuk, M. Bär, W. Ebeling, B. Lindner B, and L. Schimansky-Geier, Eur. Phys. J. Special Topics **202** 1 (2012).
[19] R. D. Groot and P. B. Warren, J. Chem. Phys. **107**, 4423 (1997).
[20] N. Goldenfeld, *Lectures on Phase Transitions and the Renormalization Group*, Forntiers in Physics Vol. 85 (Addison-Wesley, 1992).
[21] S. Ramaswamy, R. A. Simha, and J. Toner, Europhys. Lett. **62**, 196 (2003).
[22] H. Chaté, F. Ginelli, and R. Montagne, Phys. Rev. Lett. **96**, 180602 (2006).
[23] F. J. Sevilla, V. Dossetti, and A. Heiblum-Robles, J. Stat. Mech. P12025 (2014).
[24] P.-S. Shim H.-M. Chun, and J. D. Noh, arXiv:1506.06206.